NACA TN 3851

NATIONAL ADVISORY COMMITTEE FOR AERONAUTICS

TECHNICAL NOTE 3851

FAILURE CHARACTERISTICS OF PRESSURIZED STIFFENED CYLINDERS

By Roger W. Peters and Norris F. Dow

Langley Aeronautical Laboratory
Langley Field, Va.

NACA
Washington
December 1956

NATIONAL ADVISORY COMMITTEE FOR AERONAUTICS

TECHNICAL NOTE 3851

FAILURE CHARACTERISTICS OF PRESSURIZED STIFFENED CYLINDERS

By Roger W. Peters and Norris F. Dow

SUMMARY

Tests were made of stiffened cylinders of 2024 aluminum alloy under internal pressure and cyclic torsion. Fatigue cracks which developed in the skin resulted in both gradual and explosive types of failure. The types of failure depended upon the hoop stress and the structural configuration, and particularly upon the ratio of area in rings to associated skin area. Similar tests made of stiffened cylinders of both 2024 and 7075 aluminum alloys revealed that the 7075 alloy is somewhat more prone to explosive type of failure. In tests of two 7075 aluminum-alloy cylinders, explosive failures occurred without showing any signs of crack initiation before the explosion.

INTRODUCTION

The failures of pressurized fuselages that have occurred have varied greatly in severity: There have been numerous cases of minor ruptures which have been discovered and repaired before extensive damage occurred; there have been cases of sudden decompression which have caused extensive fuselage damage but which have permitted a safe landing of the aircraft (ref. 1); and there have been catastrophic failures which have completely destroyed the aircraft (ref. 2). These failures may be precipitated by punctures inflicted by projectiles, runway debris thrown upward by the landing gear during take-off or landing, broken propeller blades, collision with other aircraft, collisions with ground-maintenance vehicles, and fatigue cracks (ref. 3).

The question arises as to whether these punctures or cracks will produce a minor rupture or a catastrophic explosion. Accordingly, the Langley structures research laboratory has been engaged in a basic study of the factors which may influence the character of the failure. Two series of tests have been completed on stiffened cylinders approximately representative of fuselage construction. The first series of tests was made to determine whether explosive failure will occur. The results of the tests on the first eight cylinders of this series were presented in reference 4. The second series of tests was made to compare the character of the failures of cylinders constructed of 2024 and 7075 aluminum alloys. The purpose of this paper is to present the results of all the tests performed in these two series.

SYMBOLS

A_R	cross-sectional area of ring, sq in.
$A_{R,red}$	reduced cross-sectional area of ring (cross section at notch for longitudinal stringer), sq in.
l	ring spacing, in.
p	internal pressure, ksig
r	radius of cylinder, in.
t_S	skin thickness, in.
σ_{hoop}	nominal hoop tensile stress in skin, pr/t_S, ksi

TEST SPECIMENS

The specimens in the first series of tests were stiffened cylinders, $30\frac{3}{8}$ inches in diameter (hereinafter referred to as 30-inch cylinders), approximately representative of fuselage construction (fig. 1). Internal reinforcing consisted of longitudinal stringers and of rings riveted to the skin between the stringers. The rings were 0.051-inch spun Z-sections $1\frac{1}{4}$ inches deep, notched for the 20 stringers so that the full cross-sectional area A_R of 0.093 square inch was reduced to a value of $A_{R,red}$ of 0.053 square inch (fig. 2). The stringers were 0.040-inch-thick extruded Z-sections having a web width-thickness ratio of $12\frac{1}{2}$ and a ratio of outstanding-flange width to web height of 0.4. The cross-sectional area of the stringers was 0.045 square inch. All internal material was 2024-T4 aluminum alloy.

Six thicknesses of 2024-T3 aluminum-alloy skin varying from 0.012 to 0.040 inch were tested. These six skin thicknesses and two ring spacings, 7.5 and 15 inches, made up the primary variations in structural configuration investigated in this series of tests. The combinations of these variables are listed in table 1.

A secondary structural variation was the cutout in the center of the cylinder used as a stress-raiser to induce a fatigue crack in the cylinder. For some of the cylinders subjected to the high values of hoop tension,

a 2-inch-diameter circular cutout was used. For the lower stresses, a square cutout with 1/4-inch corner radius was used to increase the stress concentration and reduce the number of load cycles required to cause cracking. A frame around the cutout, consisting of a flange angle around the perimeter of the hole and a floating diaphragm to close the hole, was riveted on the first cylinder and was attached with screws in oversize holes on all subsequent cylinders so that the frame carried only negligible stress.

All riveting was done with 3/32-inch-diameter 2117-T3 aluminum-alloy roundhead rivets at approximately 1/2-inch pitch. Seams between sheets forming the skin were longitudinal lap joints with two rows of rivets. In addition to the double rows of rivets, an adhesive was used in all the skin seams (and only in the skin seams) in an effort to avoid seam failures.

The second series of tests was performed on cylinders having diameters of $48\frac{3}{8}$ inches (hereinafter referred to as 48-inch cylinders). Again the internal reinforcing consisted of longitudinal stringers and rings riveted to the skin between the stringers. The rings were 0.051-inch spun Z-sections 1.05 inches deep, notched for the 24 stringers so that the full cross-sectional area A_R of 0.085 square inch was reduced to a value of $A_{R,red}$ of 0.041 square inch. The longitudinal stringers were the same as those used in the 30-inch cylinders except for a slightly smaller riveted flange and a cross-sectional area of 0.043 square inch. In this series of specimens the rings were spaced at 8.0 inches. Two skin thicknesses, 0.016 and 0.025 inch, of 2024-T3 and 7075-T6 aluminum alloy were tested. In each cylinder of this series the longitudinal stringer and ring alloys were the same as the skin alloy. The combinations of these variables are listed in table 2.

In the 48-inch cylinders, four 4-inch-diameter cutouts were used as stress-raisers (fig. 3). The reinforcing around the cutout, similar to that used in the 30-inch cylinders, was attached to the skin with screws in oversize holes. Riveting of the 48-inch cylinders was identical to that of the 30-inch cylinders. Again, an adhesive was used in all skin seams.

TEST PROCEDURE

The tests were made in the combined load testing machine of the Langley structures research laboratory (ref. 5) as shown in figure 3. The torsion loading component of the machine was fitted with a cycling device to apply cyclic shear to the cylinder. Internal pressure was

supplied by oil from the hydraulic pumping unit shown in the lower right of figure 3 and was measured by the sensitive pressure indicator shown on the right. The combination of cyclic shear and internal pressure induced stress conditions adjacent to the cutout in the test cylinder which were not greatly dissimilar from those adjacent to a cutout in the side of a pressurized cabin in flight, except that in the test cylinder the magnitude of the shear stress was intentionally exaggerated to minimize the number of cycles required to induce a fatigue crack.

The procedure in each test (except for 30-inch cylinder 10) was to increase the internal pressure until the desired nominal hoop tensile stress was attained. While the internal pressure was being increased, the axial loading component of the testing machine was operated simultaneously to maintain zero external axial load on the cylinder and thereby obtain the free cylinder axial stress equal to half the hoop stress. When the desired nominal hoop tensile stress had been attained, the internal pressure was maintained constant and completely reversed cyclic torsion was applied until a crack opened at the cutout. The internal-pressure controls were manipulated to maintain the constant pressure within the cylinder despite the growing leakage through the lengthening crack. When the crack length became such that the leakage of oil from the crack exceeded the discharge capacity of the hydraulic pumping unit and the internal pressure could no longer be maintained, the test was terminated. In the tests of the 30-inch cylinders the available pumping capacity of approximately 8 gallons per minute permitted a maximum crack length of approximately 3 inches. For the tests of the 48-inch cylinders a larger pumping unit having a capacity of 32 gallons per minute was obtained which permitted maximum crack lengths of approximately $6\frac{1}{2}$ inches. In tests of cylinders 13 and 16, the magnitude of the cyclic shear stress was halved after initiation of the crack to slow the crack growth.

Cylinder 10 was tested by the following procedure: Internal pressure was applied and held constant to produce a hoop tensile stress of 20 ksi. While this stress was maintained, cyclic torsion producing a shear stress of ±12.1 ksi was applied. A crack appeared after 353 cycles and had grown to a length of approximately $\frac{3}{4}$ inch at $363\frac{1}{2}$ cycles. The torsion was then reduced to zero and internal pressure was cycled manually to produce a cyclic hoop tensile stress varying from 3.8 to 20 ksi. After 50 pressure cycles the crack had not grown appreciably. While internal-pressure cycling was continued between 3.8 and 20 ksi, torsion was cycled to produce a shear stress of ±1.2 ksi. After 2,061 shear cycles at ±1.2 ksi and 20 additional pressure cycles, there was still no increase in crack growth. Accordingly, the shear stress was increased to ±2.4 ksi and internal-pressure cycling was continued. After 1,012 shear cycles at ±2.4 ksi and 15 additional pressure cycles, crack growth was still less than 1/16 inch. When torsion was cycled at a shear stress of ±4.8 ksi

and internal pressure cycling was continued as before, the crack length grew gradually to 2.4 inches. At this crack length it was impossible to attain the pressure required to produce a hoop tensile stress of 20 ksi. At the termination of the test, 1,880 shear cycles at ±4.8 ksi and 51 additional pressure cycles for a total of 136 pressure cycles had been attained.

RESULTS AND DISCUSSION

30-Inch Cylinders

The results of the tests on the 30-inch cylinders are presented in table 1. Two distinct modes of failure occurred: One was characterized by a gradual crack growth (see fig. 4) in which the crack slowly grew to such length that the test was terminated at the limit of the hydraulic pumping capacity; the other is described as an explosive failure in which the crack, after growing a short distance, opened suddenly over one or more bay widths, and failed the ring at one of its notches or tore the skin away from the ring (see fig. 5).

From the results in table 1 it may be observed that the hoop stress level was not the sole cause of the difference between the modes of failure. For example, cylinders 4 and 9 experienced a gradual crack growth at a higher hoop stress level (30 ksi) than that for cylinders 3 and 12 (20 and 22.5 ksi, respectively) which had explosive failures.

Further observation of the results in table 1 shows that the number of shear-stress cycles between initial cracking and explosive failure was generally small, whereas a somewhat larger number of cycles was required in cases of gradual failures to open the crack sufficiently to necessitate termination of the test. Exceptions to this observation are cylinders 5, 7, and 11 in which only about 50 additional shear-stress cycles were required to open the crack to such an extent that pressure could not be maintained. Because the rate of crack growth in cylinders 5, 7, and 11 in terms of the number of shear-stress cycles was similar to that in cylinder 6 which had an explosive failure, the possibility exists that these cylinders might also have encountered an explosive failure if a somewhat greater pumping capacity had been available to permit continuation of the test. However, close comparison of the cracks shown in figures 4 and 5 reveals that, in all instances, the cracks developed in the cylinders having a gradual failure (fig. 4) were much longer than the cracks developed in the explosive cylinders before explosive failure (fig. 5).

These data on the tests of the 30-inch cylinders are also presented in figure 6 in which the hoop tensile stress σ_{hoop} induced by the

internal pressure is plotted against the reinforcement ratio - the ratio of the cross-sectional area in the rings $A_{R,red}$ to the associated skin area lt_S (ref. 4). The ×-points represent those cylinders which failed explosively and the circles represent cylinders which experienced a gradual crack growth. The numbers adjacent to the test points refer to the cylinders listed in table 1. The test points tend to establish a pattern which permits drawing a boundary, such as that shown by the dashed curve, between the regions of explosive and nonexplosive failures. The boundary shown is considered valid only for cylinders of 2024 aluminum alloy having stringers and notched rings riveted directly to the skin.

48-Inch Cylinders

The results of the tests on the 48-inch cylinders to compare the failure characteristics of 2024 and 7075 aluminum alloys are presented in table 2. As noted in the previous series of tests, two modes of failure occurred. Cylinder 15, constructed of 7075 aluminum alloy, experienced an explosive failure; whereas cylinders 13 and 17, constructed of equal thicknesses of 2024 aluminum alloy and tested at the same nominal hoop tensile stress (30 ksi), failed in a gradual manner. A similar comparison exists between cylinder 19 (7075 aluminum alloy) and cylinder 18 (2024 aluminum alloy) which were tested at σ_{hoop} = 25 ksi. Cylinders 16 and 14 (7075 and 2024 aluminum alloys, respectively), which were tested at σ_{hoop} = 20 ksi, both failed in a gradual manner.

The explosive failures of cylinders 15 and 19, however, differed from the explosive failures previously described in that the explosions occurred without any visible signs of crack initiation prior to the failure. A comparison of the failures of cylinders constructed of these aluminum alloys is illustrated in figure 7.

The data from the tests of all the 48-inch cylinders are presented in figure 8 in which the nominal hoop tensile stress is plotted against the reinforcement ratio $\frac{A_{R,red}}{lt_S}$. The cylinders of 7075 aluminum alloy which experienced explosive failure are represented by asterisks, and the cylinders of 2024 and 7075 aluminum alloy which experienced gradual failure are represented by the circles and squares, respectively. The boundary established in figure 6 by the tests of the 30-inch cylinders is drawn on this figure for comparison. The number of explosive-failure points for the cylinders of 7075 alloy falling below this curve indicate that the boundary established from tests of 2024 cylinders may be somewhat high for cylinders constructed of the more explosive-prone 7075 alloy.

Effect of Pressurizing Medium

The question arises as to whether the results obtained from tests of cylinders pressurized with oil (or water) are indicative of the behavior of cylinders pressurized by air. Altitude-chamber tests and water-tank tests on box structures (ref. 6) indicated very little difference between the two pressurizing mediums. A limited number of tests on unstiffened cylinders having precut slits and pressurized by both oil and air indicate that the pressure required to cause failure is virtually the same whether oil or air is used. Preliminary results by another investigator on similar cylinders pressurized by oil, water, and air also indicate that the pressures sufficient to cause failure are the same regardless of the pressurizing medium. However, both investigations show that the destructiveness of the failure is very much greater when the cylinder is air pressurized. Accordingly, it seems reasonable to expect that tests using air as the pressurizing medium would show, at most, only a slight downward shift of the boundary shown in figure 6.

CONCLUDING REMARKS

Tests of pressurized stiffened cylinders of 2024 aluminum alloy have shown that if a crack is opened in the skin of such a structure it may grow in either a gradual or an explosive manner depending upon the structural configuration as well as upon the stress conditions imposed on the structure. For the type of construction tested in this series, that is, for cylinders having notched rings riveted to the skin, a boundary can be drawn between explosive and nonexplosive failures. This boundary is shown to be dependent on the reinforcement ratio - the ratio of area in the rings to the associated skin area.

Tests on a series of pressurized stiffened cylinders of 2024 and 7075 aluminum alloys have shown that the 7075 alloy is somewhat more prone to explosive type of failure than the 2024 alloy. In tests of two 7075 aluminum-alloy cylinders explosive failures occurred without showing any signs of crack initiation before the explosion.

Langley Aeronautical Laboratory,
National Advisory Committee for Aeronautics,
Langley Field, Va., August 28, 1956.

REFERENCES

1. Civil Aero. Board: Resume of U.S. Air Carrier Accidents (Calendar Year 1950). Aug. 1951.

2. Anderton, David A.: RAE Engineers Solve Comet Mystery. Aviation Week, vol. 62, no. 6, Feb. 7, 1955, pp. 28-30, 34, 37, 39, 40, 42.

3. Hitchcock, L. M.: High-Altitude Cabin-Pressurization Design Criteria Related to Future Transport Operations. Aero. Eng. Rev., vol. 14, no. 8, Aug. 1955, pp. 44-49.

4. Dow, Norris F., and Peters, Roger W.: Preliminary Investigation of the Failure of Pressurized Stiffened Cylinders. NACA RM L55D15b, 1955.

5. Peters, R. W.: The NACA Combined Load Testing Machine. Proc. Soc. Exp. Stress Analysis, vol. XIII, no. 1, 1955, pp. 181-198.

6. Anon.: Tests Show Comet Fuselage Stronger. Aviation Week, vol. 65, no. 8, Aug. 20, 1956, pp. 72, 73.

TABLE 1

STRUCTURAL CONFIGURATIONS, LOADING CONDITIONS, AND RESULTS OF TESTS OF 30-INCH CYLINDERS

[2024 aluminum alloy]

Cylinder	Cutout	Skin thickness, t_s, in.	Ring spacing, l, in.	$\frac{A_{R,red}}{l t_s}$	Hoop tensile stress, σ_{hoop}, ksi	Applied cyclic shear stress, ksi	Number of cycles to initiate crack	Number of cycles at end of test	Type of failure
1	Square	0.040	15.0	0.09	20	±14.1	1,261	1,263	Explosive[a]
2	Square	.012	7.5	.59	20	±12.1	281	528	Gradual
3	Square	.040	15.0	.09	20	±14.1	136	147.5	Explosive
4	Round	.012	7.5	.59	30	±12.1	658	875	Gradual
5	Square	.040	15.0	.09	10	±12.1	203.5	255.5	Gradual
6	Round	.016	7.5	.44	40	±12.1	728	788	Explosive
7	Square	.032	7.5	.22	22.5	±12.1	194	234	Gradual
8	Square	.025	7.5	.28	30	±12.1	5	13	Explosive
9	Square	.020	7.5	.35	30	±12.1	582	695	Gradual
10	Square	.040	7.5	.18	20	±12.1	353	(b)	Gradual
11	Square	.040	15.0	.09	15	±12.1	317	370	Gradual
12	Square	.025	15.0	.14	22.5	±12.1	280	293.5	Explosive

[a]The first cylinder failed in the seam between two pieces of skin.
[b]See discussion in text of revised test procedure for cylinder 10.

TABLE 2

STRUCTURAL CONFIGURATIONS, LOADING CONDITIONS, AND RESULTS OF TESTS OF 48-INCH CYLINDERS

[l = 8.0 inches]

Cylinder	Aluminum alloy	Skin thickness, t_s, in.	$\frac{A_{R,red}}{l t_s}$	Hoop tensile stress, σ_{hoop}, ksi	Applied cyclic shear stress, ksi	Number of cycles to initiate crack	Number of cycles to end of test	Type of failure
13	2024	0.015	0.35	30	±12.1 ±6.0	72 ---	88 1,642	Gradual
14	2024	.025	.21	20	±12.1	178	210	Gradual
15	7075	.016	.32	30	±12.1	34	34	Explosive[a]
16	7075	.025	.21	20	±12.1 ±6.0	229 ---	229 1,899	Gradual
17	2024	.015	.35	30	±12.1	129	174	Gradual
18	2024	.025	.21	25	±12.1	56	69	Gradual
19	7075	.025	.21	25	±12.1	256	256	Explosive[a]
20	7075	.016	.25	25	±12.1	113	117	Explosive

[a]Cylinders 15 and 19 exploded without any visible signs of crack initiation prior to the failure.

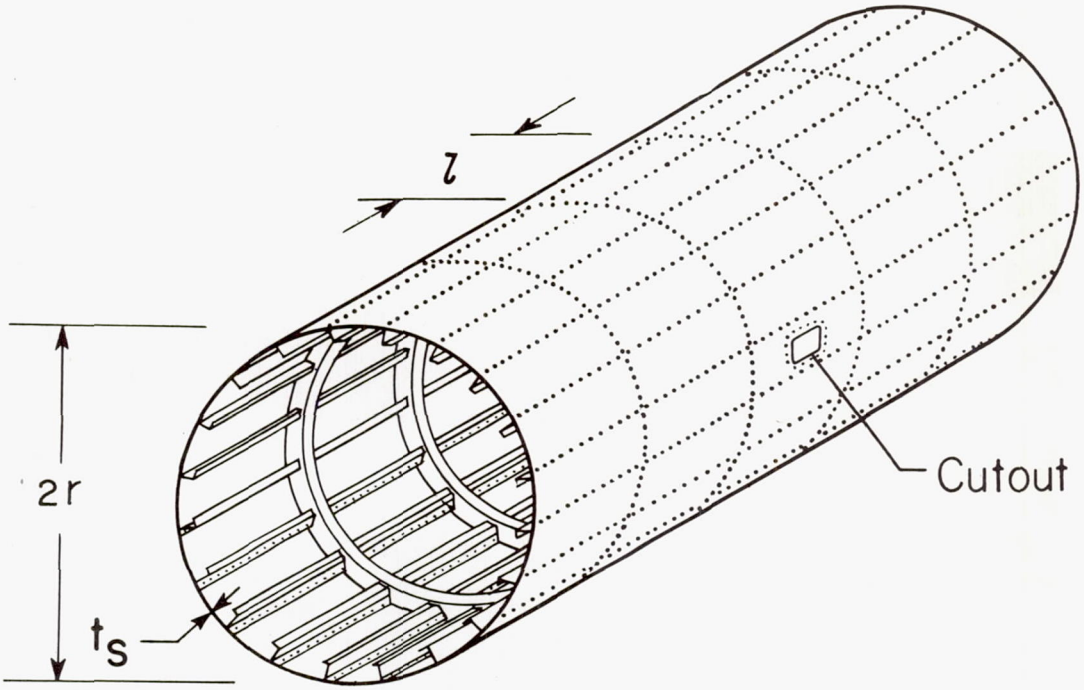

Figure 1.- Construction of test cylinders.

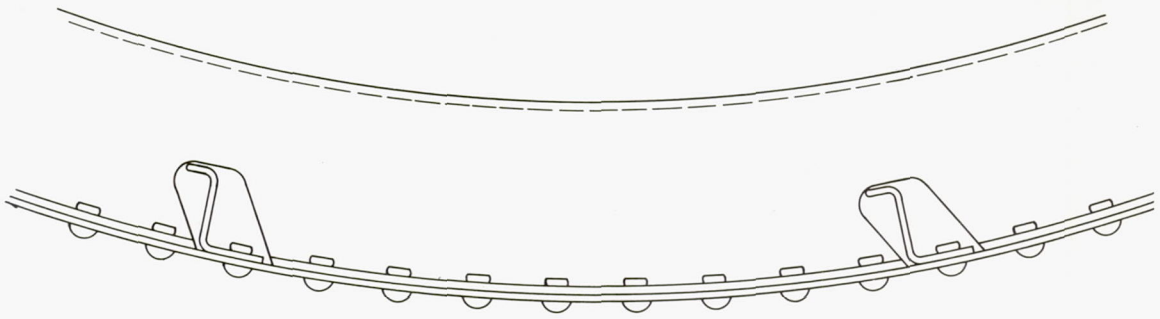

Figure 2.- Detail of ring installation.

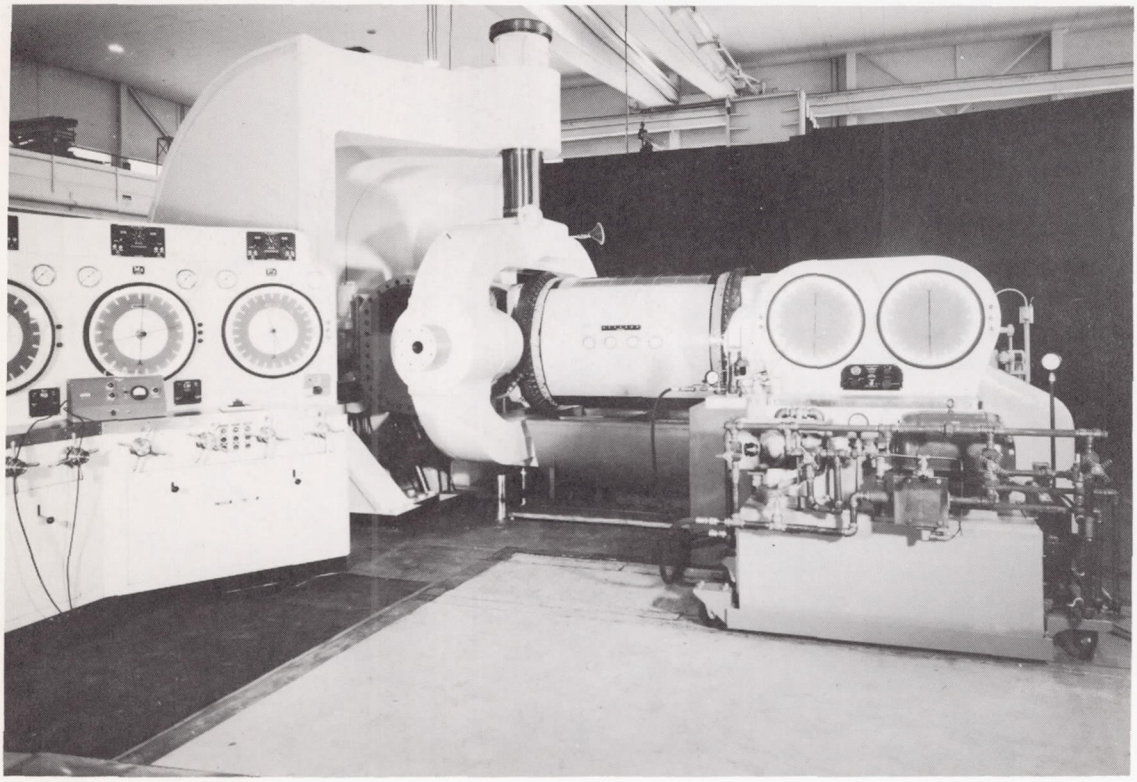

L-92104

Figure 3.- Setup of 48-inch cylinder in combined load testing machine. (Oil-salvaging cover is removed to show test cylinder.)

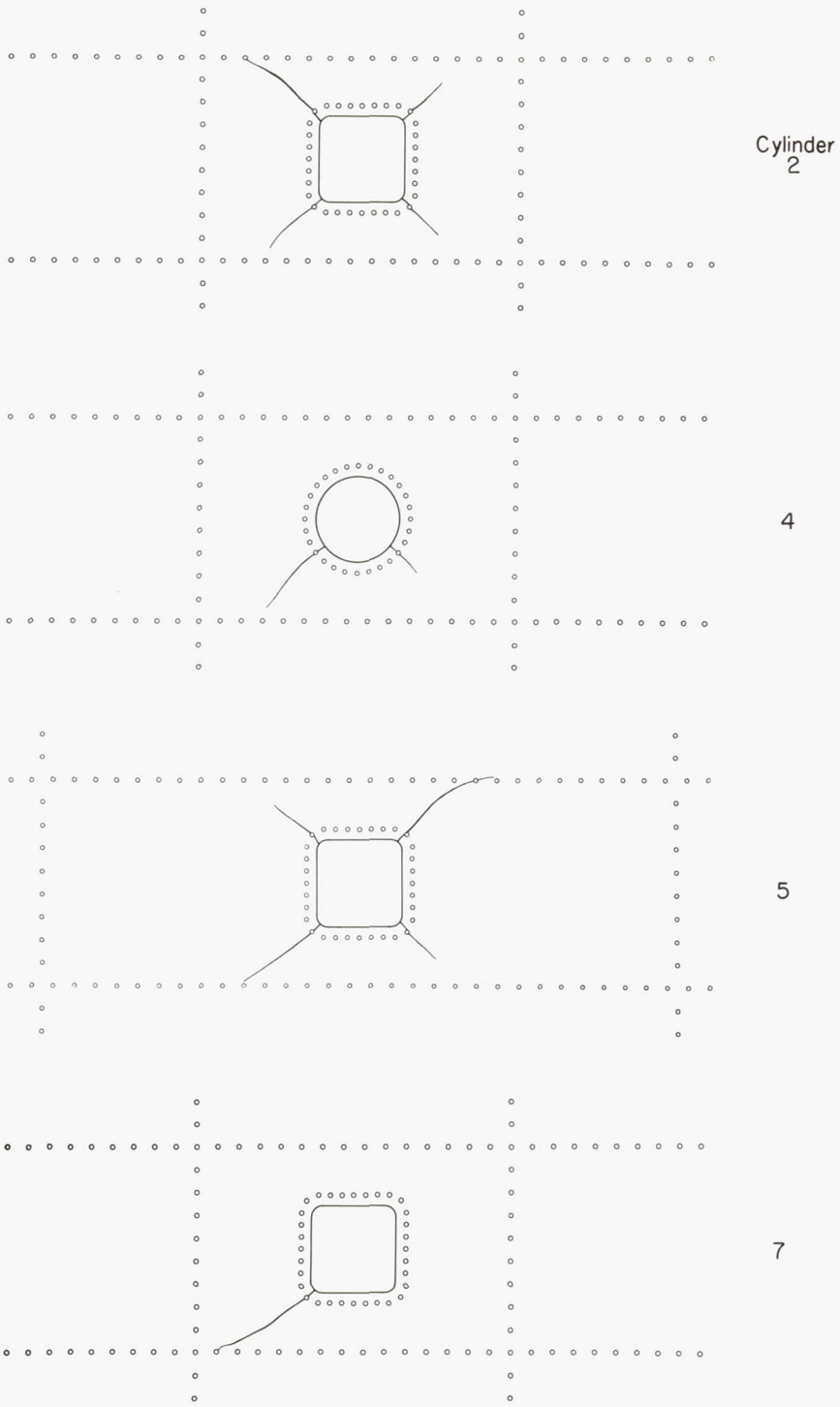

Figure 4.- Final cracks in 30-inch cylinders having gradual failure.

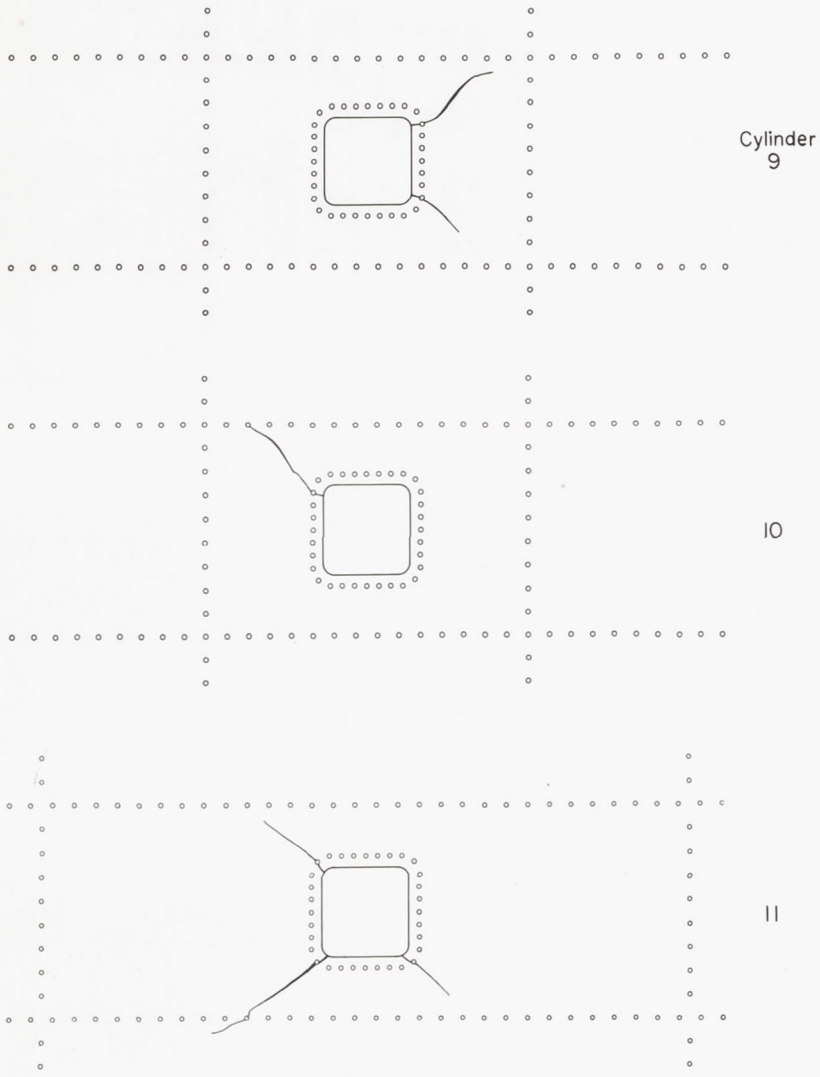

Figure 4.- Concluded.

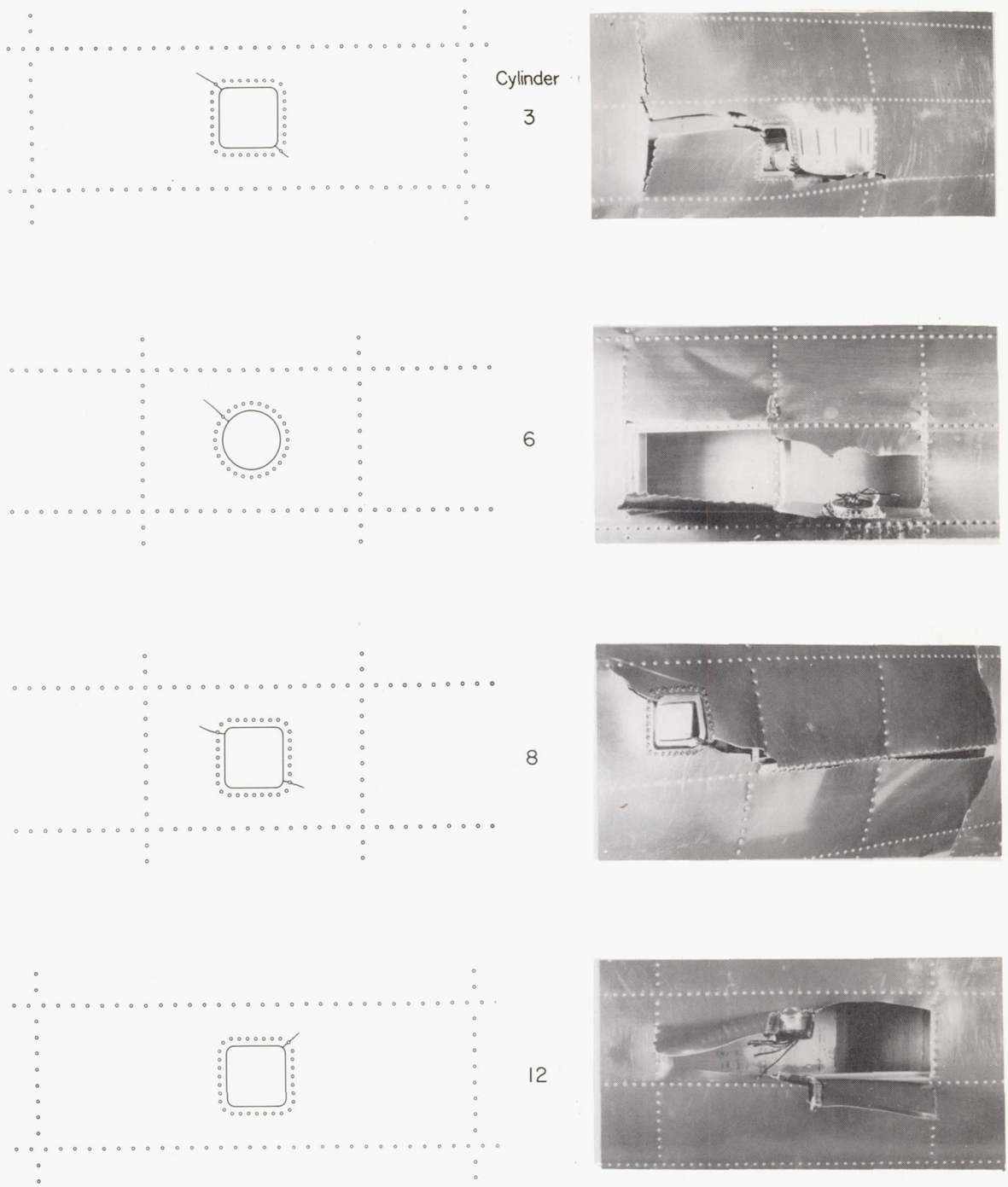

L-95811

Figure 5.- Cracks before and after explosive failure in 30-inch cylinders.

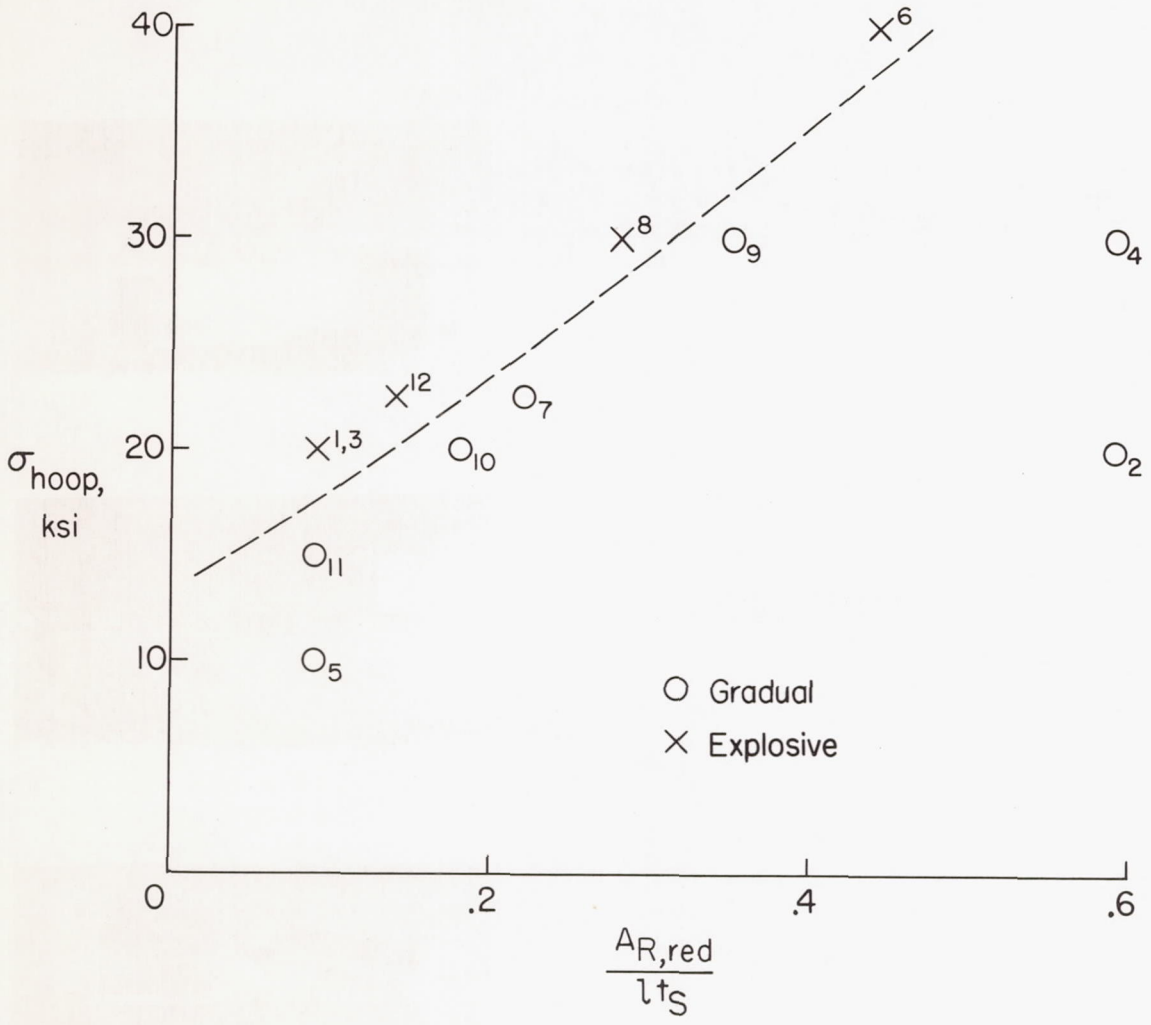

Figure 6.- Regions of explosive and gradual crack growth as determined by tests of 30-inch stiffened cylinders of 2024-T3 aluminum alloy.

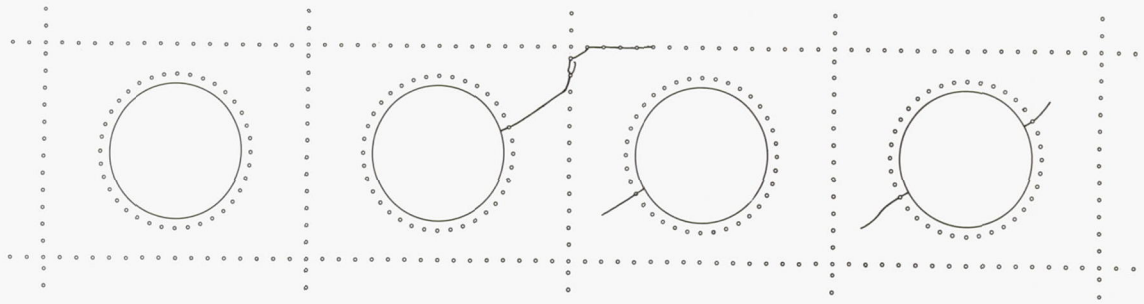

(a) Cylinder 13; σ_{hoop} = 30 ksi; t_s = 0.015 inch 2024 aluminum alloy.

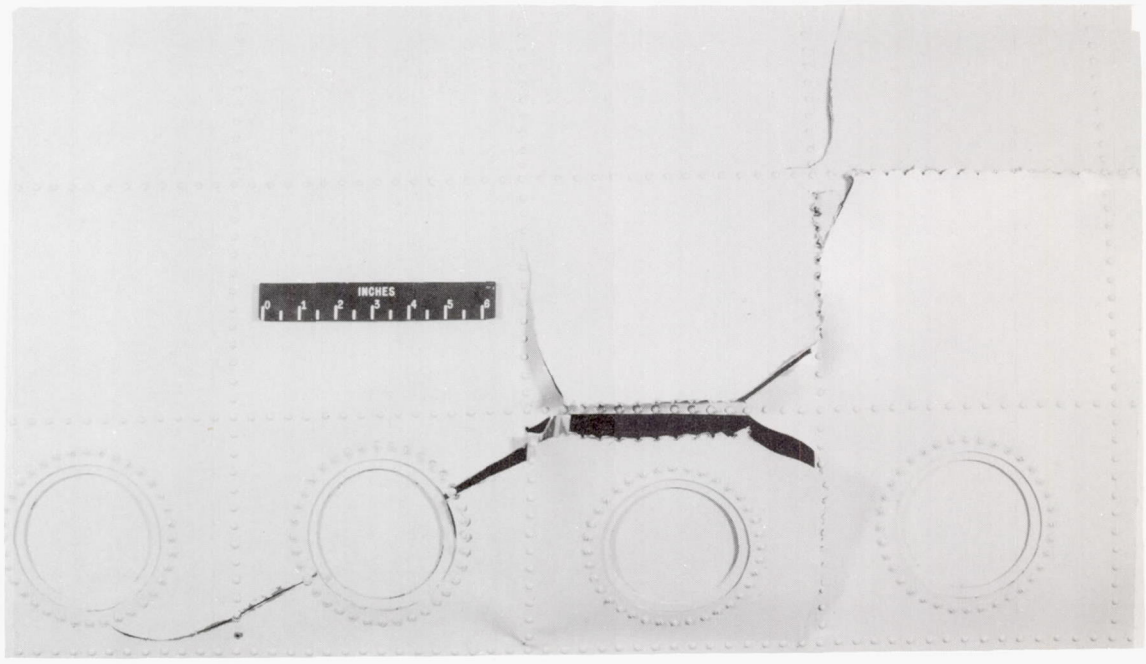

L-95812

(b) Cylinder 15; σ_{hoop} = 30 ksi; t_s = 0.016 inch 7075 aluminum alloy.

Figure 7.- Comparison of failures of 2024 and 7075 aluminum-alloy cylinders.

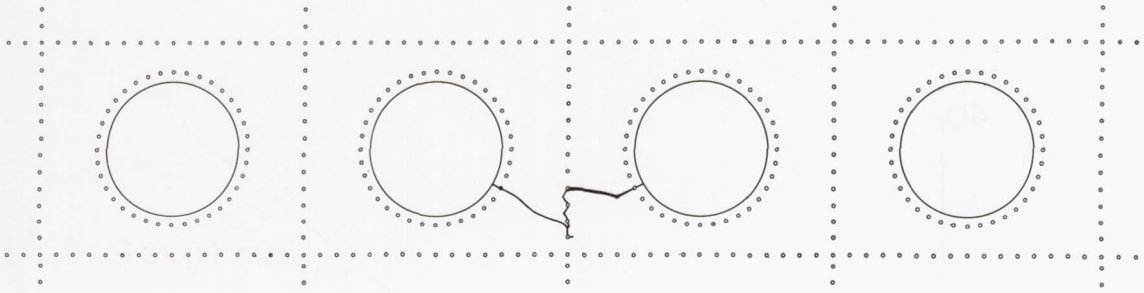

(c) Cylinder 18; σ_{hoop} = 25 ksi; t_s = 0.025 inch 2024 aluminum alloy.

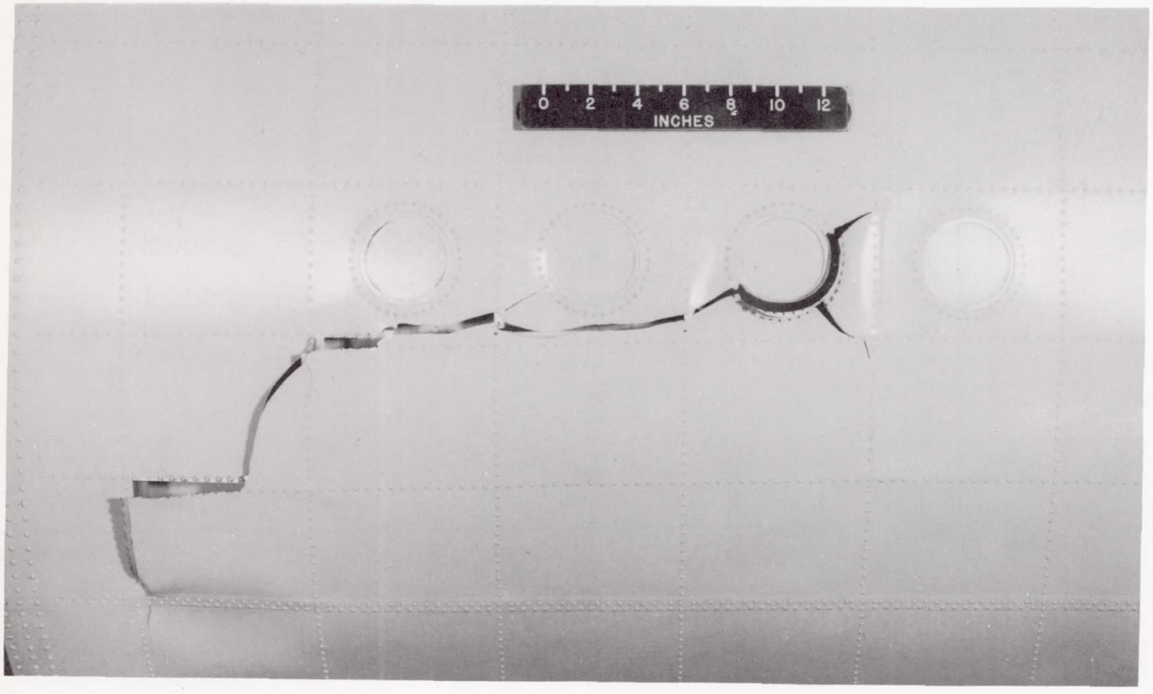

L-9581

(d) Cylinder 19; σ_{hoop} = 25 ksi; t_s = 0.025 inch 7075 aluminum alloy.

Figure 7.- Concluded.

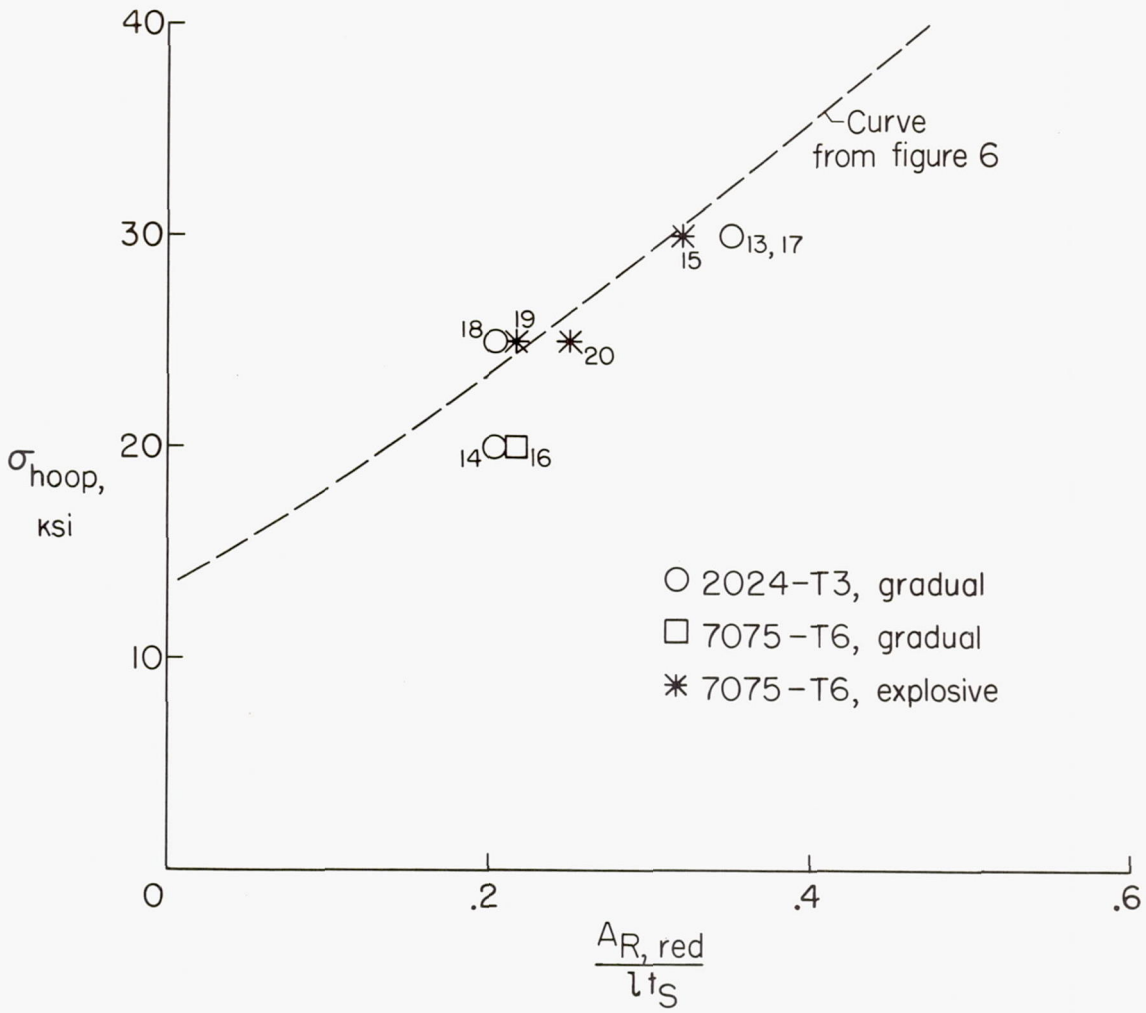

Figure 8.- Explosive and gradual crack growth as determined by tests of 48-inch cylinders of 2024-T3 and 7075-T6 aluminum alloy.